

Influence of Bismuth Dopant on Physical Properties of nanostructured TiO₂ Thin Films

Oday Mazin Abdulmunem¹, Firas S. Abdulameer¹, Haider A. Kadhum¹, Mohammed Odda Dawood¹, Khalid Haneen Abass², Nadir Fadhil Habubi³, Sami Salman Chiad^{3*}.

¹Department of Physics, College of Science, Mustansiriyah University, Baghdad, Iraq.
munem@uomustansiriyah.edu.iq, firasalaraji@uomustansiriyah.edu.iq, haider_mu2017@uomustansiriyah.edu.iq, mohammedodda2017@uomustansiriyah.edu.iq.

²Department of Physics, College of Education for Pure Sciences, University of Babylon, Iraq,
pure.khalid.haneen@uobabylon.edu.iq.

³Department of Physics, College of Education, Mustansiriyah University, Baghdad, Iraq,
nadirfadhil@uomustansiriyah.edu.iq, dr.sami@uomustansiriyah.edu.iq.

*Corresponding author. E-mail: dr.sami@uomustansiriyah.edu.iq.

Article Info

Volume 83

Page Number: 11142 - 11147

Publication Issue:

March - April 2020

Article History

Article Received: 24 July 2019

Revised: 12 September 2019

Accepted: 15 February 2020

Publication: 13 April 2020

Abstract:

Nano structured TiO₂ was prepared utilizing spray pyrolysis deposition (SPD). The characterization of the deposited films was studied with Bi dopant. The XRD analysis indicated that films are polycrystalline with a preferred orientation along (110) direction. The AFM analysis shows a porous morphology structure. The optical properties were obtained by UV-visible spectro photometer, which show that these films were highly transparent above 80% at the wavelength more than 700 nm with a slightly influenced upon Bi content. The energy gap was shifted from 3.1 to 2.6 eV, versus doping.

Keywords: Bi:TiO₂, SPD, Optical, structure, topographical.

I. INTRODUCTION

Titanium oxide (TiO₂) is a n-type semiconductor with wide energy bandgap of 3.2. TiO₂ show pleasant properties like transparency to visible light, high refractive index and a low absorption coefficient. [1-3]. TiO₂ has three main crystalline structures: anatase (tetragonal), brookite (orthorhombic) and rutile (tetragonal). Rutile is commonly stable at high temperatures [4]. The phase conversion from anatase to rutile relies on film growth process, which might be influenced by defect concentration, grain boundary concentration, and particle packing [5, 6]. It is found that the optical properties and electronic structure of TiO₂ is modified under the doping of transition elements. These transition metals minimize the rate of recombination of hole-electron pairs, and improve the “interfacial

charge transfer efficiency” [7,8]. There are several TiO₂ thin film deposition techniques including sol-gel deposition [9], spray pyrolysis [10], pulsed laser deposition [11], e-beam evaporation [12], chemical vapor deposition [13], and reactive magnetron sputtering [14]. In this paper pure Titanium dioxide and doping with Bismuth 2% and 4% thin films prepared in the simple and low cost of CSP in order to study their optical, structural and Morphology.

II. EXPERIMENTAL

Titanium dioxide (TiO₂) and Bismuth (Bi) -doped TiO₂ thin films were prepared by CSP method. The aqueous solution containing 0.05 M of Titanium acetate (Ti (CH₃COO)₂·2H₂O) and 100 mL of deionized water was used to obtain the matrix solution. To prepare the doping material

0.1M of cupric nitrate trihydrate (Bi(NO₃)₂.3H₂O) to dissolve in deionized water of dopant as a volumetric percentage 2 and 4., which kept constant during the deposition process for TiO₂ and Bi doped TiO₂. Substrate temperature was kept at 450°C during deposition process. Nitrogen was used as a carrier gas, distance between substrate and nozzle was kept at 29 cm. spraying time, spraying rate and the time interval between two spray process were 8 s, 5m L/min and 1 min respectively.

Film thickness was obtained by Gravimetric technique and was about 350± 30 nm. Transmittance and Absorbance spectra were recorded via Shimadzu double beam spectrophotometer. Structural parameters were analyzed by X-ray diffractometer (Shimadzu, model: XRD-6000, Japan) using CuKα radiation. AFM (AA 3000 Scanning Probe Microscope) was utilized to study deposited thin films surface.

III. RESULTS AND DISCUSSION

XRD patterns of pure and Bi doped TiO₂ thin films are displayed in Fig. 1. The films exhibit polycrystalline tetragonal crystal structure. The diffraction peaks observed in XRD patterns of all the films corresponds to (110), (200), (201) and (203) planes of the typical tetragonal crystal structure of TiO₂ thin films compared with JCPDS card no 00-021-1236. The diffraction peaks were indexed to srilankite planes and Bi relative peaks were not observed implying that

Bi was doped into TiO₂ lattice. At doping of Bi the intensity of (110) plane increases which may be due to increase in the mobility of titanium and oxygen atoms which led to the increase in the nucleation of crystallization phase of srilankite TiO₂. The crystallite size (*D*) of the sample was calculated from full width at half maximum (FWHM) β of the (110) peak of anatase TiO₂ by Debye Scherrer equation [15, 16].

$$D = \frac{0.9 \lambda}{\beta \cos \theta} \quad \text{--- --- --- 1}$$

Where λ (1.54060 Å) is X-ray wavelength. The Dislocation density (δ) was calculated by using relation [17]:

$$\delta = \frac{1}{D^2} \left(\frac{\text{lines}}{m^2} \right) \quad \text{--- --- --- 2}$$

The micro strains (ε) were caused by crystalline defects and determined using the following relation 3 [17, 18]:

$$\epsilon = \frac{\beta \cos \theta}{4} (\text{lines}^{-2} \cdot m^{-1}) \quad \text{--- --- --- 3}$$

The variation of *D* and lattice parameters with dopant Bi was calculated and the findings are recorded in Table 1, which assure that *D* full in the category of nano. The Crystallite size of the plane (110) increases with the increase of concentration doping of Bi. Their proving in the crystallinity of the films are confirms decreasing in defects. This also confirms from the grain size, which is increased by increasing the concentration doping in Bi.

Table 1: Structural data of TiO₂ with different Bi doping by (SPD).

Bi (%)	(hkl)	2θ	Lattice constant	FWHM		(ε)	(δ)
Doping	Plane	(Deg.)	(Å)	(Deg.)	D (nm)	×10 ⁻⁴	(Line. m ⁻²) ×10 ¹⁵

0	-110	24.93	a	b	c	0.88	9.17	38.64	11.883
			5.45	9.18	5.14				
2	-110	24.93	a	b	c	0.86	9.41	37.64	11.277
			5.45	9.18	5.14				
4	-110	24.93	a	b	c	0.8	10.05	35.24	9.883
			5.45	9.18	5.14				

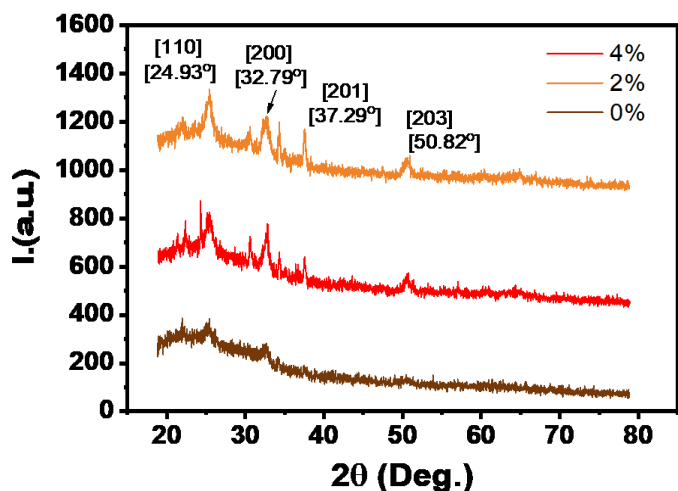


Figure 1. XRD pattern of pure TiO₂ films and 2% and 4% Bi doping concentrations.

The surface morphologies of pure TiO₂ and different concentration Bi doping films are illustrated in Fig. 2. The surface morphology of the pure TiO₂ film was composed of different grain size with average diameter 92.44 nm, average roughness (Ra) 1.07 nm and the root mean square (R. M. S) 1.3 nm. In addition, it was found that the films deposited at 2 % and 4 % Bi doping were increase slightly in average diameter (97.45-123.47) nm, Ra and R. M. S were getting the same behaviors in addition to that some grains was sharp as shown in Fig. 2. The increased values of Ra and RMS of the films, indicating its good polycrystalline structure at the surface make these films suitable in solar cell applications [19]. The R.M.S and average roughness (R_a) of prepared films are shown in Table 2. As can be seen the R_{rms} and R_a follow the dopant.

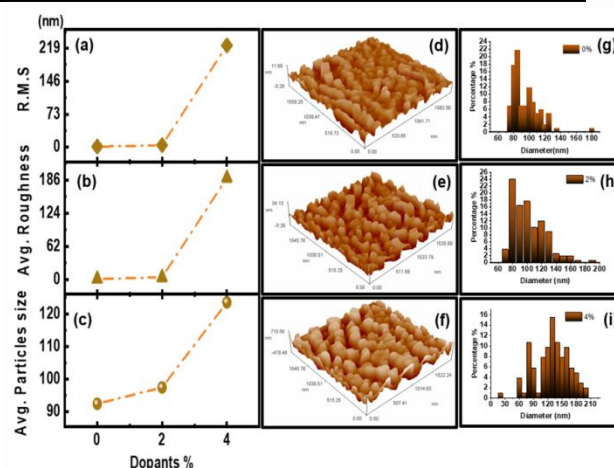


Figure 2. a. AFM image of pure TiO₂ thin films. e. and f. AFM images of the doped Bi: TiO₂ 2% and 4%.

Table 2: surface morphology of TiO₂ with different Bi doping by (SPD).

mn doping (%)	Avg. Diameter (nm)	R _a (nm)	R. M. S. (nm)
0	92.44	1.07	1.3
2	97.45	4.07	4.64
4	123.47	19	22.5

Transmittance spectra of the films are obtained by UV-Vis spectrophotometer in the wavelength range between 200 to 900 nm Fig.3. It is clear that when the concentration doping increases then transmittance slightly decreases. The films show high transmittance above 80% at wavelength more than 700 nm. Since the calculated energy band gaps of pure films are approximately 3.1 eV. Therefore, these films absorb photons with wavelength less than 400 nm, according to the

relation $\lambda(\text{nm}) = 1240/E_g(\text{eV})$. All these films show high absorption in the wavelength below than 600nm.

When the wavelength of light increased from 550nm, then its transmittance increases. Upto 600nm, the maximum obtained transmittance is 80%. Therefore, these films can be used for the protection of optoelectronic devices from UV radiations.

The absorption coefficient (α) for each wavelength was calculated from equation (4) [20]:

$$\alpha = 2.303(A/T) \quad \text{--- 4}$$

Fig. 4 shows absorbance spectra of the deposited samples. It was clear that absorbance increased via increase Bi content, and that films after doping have values of absorption coefficient ($\alpha > 10^4 \text{ cm}^{-1}$) this means that the direct transition is possible to occur. Bi dopant altered local lattice symmetry and defect, which could modulate absorbance and material properties[21].

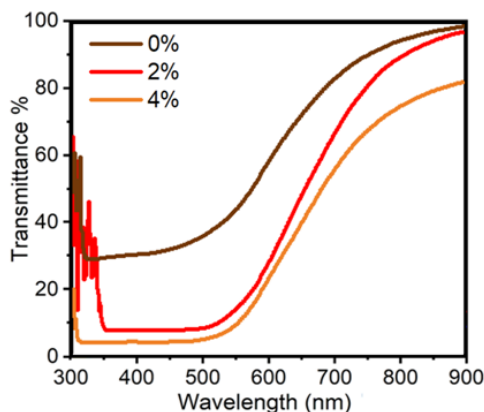


Figure 3. Transmittance with wavelength of pure and 2% and 4% Bi: TiO₂ thin films.

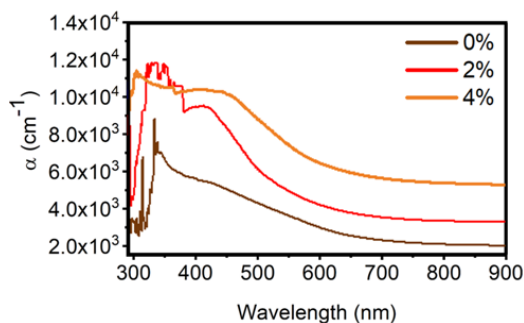


Figure 4. Absorption coefficient with wavelength of pure and 2% and 4% Bi:TiO₂ thin films.

The optical energy bandgap of pure TiO₂ and doped Bi thin films are calculated by the following Tauc's relation [22, 23].

$$(\alpha h\nu) = A(h\nu - E_g)^n \quad \text{--- 5}$$

Where n equal to 1/2 or for direct transition. A is a constant quantity, E_g is the bandgap energy, $h\nu$ is photon energy. Optical bandgap energy is determined by plotted a graph between $h\nu$ and $(\alpha h\nu)^2$ as shown in Fig. 5. The calculated bandgap energy for pure TiO₂ and doped of Bi 2% and 4% thin films are 3.1, 2.8 and 2.6 eV, respectively. This decrease bandgap is due to the increase in doping of the films which is according to the literatures [25-27].

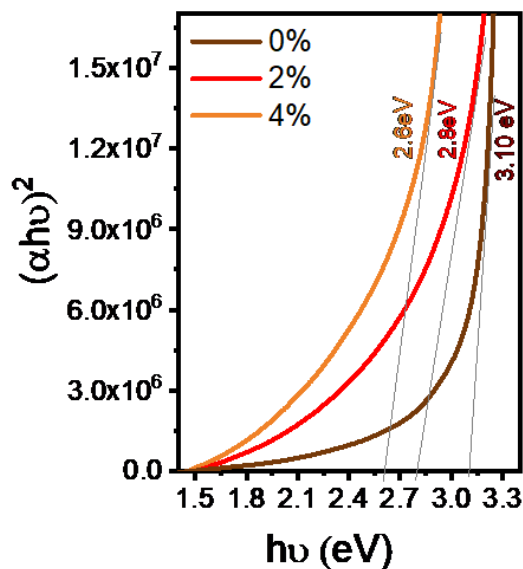


Figure 5. Indirect bandgaps of pure and 2% and 4% Bi: TiO₂ thin films.

IV. CONCLUSIONS

The structure, optical properties, and surface morphology of nanostructure TiO₂ and different Bi dopant concentrations films deposited by CSP were investigated. XRD results display polycrystalline structure. All films show high transmittance above 80% in the visible region.

Bandgap decrease with increase in doping of films. The films deposited at 2% and 4% Bi doping were increase slightly in average diameter (97.45-123.47) nm. The Ra and R. M. S follow the average diameter.

V. ACKNOWLEDGMENTS

Authors appreciate Mustansiriyah University for their support in this work.

REFERENCES

- [1] T.L. Chen, Y. Furubayashi, Y. Hirose, T. Hitosugi, T. Shimada, T. Hasegawa, J. Phys. D: Appl. Phys. 40:5961(2007).
- [2] O.V. Sakhno, L.M. Goldenberg, J. Stumpe, T.N. Smornova, Nanotechnology18:105704(2007).
- [3] Khalid Haneen Abass, Mohammed H. Shinen, and Ayad F. Alkaim, "Preparation of TiO₂ Nanolayers via Sol-Gel Method and Study the Optoelectronic Properties as Solar Cell Application", Journal of Engineering and Applied Sciences, Vol.13, No.22, pp.9631-9637, 2018.
- [4] W. Li , C. Ni, H. Lin , C. P. Huang, S. Ism at Shah: "Size dependence of thermal stability of TiO₂ nanoparticles" Journal of Applied Physics, Vol 96, No 11, pp.6663-6668(2004).
- [5] D.J. Reidy, J.D. Holmes, M.A. Morris, J. Eur. Ceram. Soc. 26:1527 (2006).
- [6] K.P. Kumar, K. Keizer, A.J. Buggraaf, T. Okubo, H. Nagamoto, J. Mater. Chem.3:1151(1993).[7] C. Zhao, A. Krall, H. Zhao, Q. Zhang, Y. Li, International Journal of Hydrogen Energy 37, 9967(2012). [8] Y. Wu, G. Lu, S. Li, J. Phys. Chem. C 113, 9950–9955 (2009). [9] M. Morozova, P. Kluson, J. Krysa, Ch. Gwenin, O. Solcova, J Sol-Gel Sci Technol. 58:175(2001).
- [10] C. Natarajan, N. Fukunaga, G. Nogami, (1998) Thin Solid Films. 322:6.
- [11] Terashima Masahiro, Inoue Narumi, Kashiwabara Shigeru, Fujimoto Ryozo, Appl. Surf. Sci. 169–170:535(2001).
- [12] Sun Lianchao, Hou Ping, Thin Solid Films, 455–456:525(2004). [13] Sun Hongfu, Wang Chengyu, Pang Shihong, Li Xiping, Tao Ying, Tang Huajuan, Liu Ming, J. Non-Cryst. Solids 354:1440(2008).
- [14] S. Boukrouh, R. Bensaha, S. Bourgeois, E. Finot, M.C. Marco de Lucas, Thin Solid Films 516:6353(2008).
- [15] B.D. Cullity, Elements of X-Ray Diffraction, 1st ed. Addison-Wesley, New York, pp.110-111(1956).
- [16] Ehssan S Hassan, Tahseen H Mubarak, Khalid H Abass, Sami S Chiad, Nadir F Habubi, Maher H Rahid, Abdulhussain A Khadayeir, Mohamed O Dawod, and Ismaeel A Al-Baidhany, "Structural, Morphological and Optical Characterization of Tin Doped Zinc Oxide Thin Film by (SPT)", Journal of Physics: Conference Series, 1234 (2019).
- [17] D. Hazel Book Comparing Strain Gage Measurements to Force Calculations in a Simple Cantilever Beam (2016).
- [18] Abdulhussain A Khadayeir, Ehssan S Hassan, Sami S Chiad, Nadir F Habubi, Khalid H Abass, Maher H Rahid, Tahseen H Mubarak, Mohamed O Dawod, and Ismaeel A Al-Baidhany, "Structural and Optical Properties of Boron Doped Cadmium Oxide", Journal of Physics: Conference Series, 1234 (2019).
- [19] Khalid Haneen Abass and Musaab Khudhur Mohammed, "Fabrication of ZnO:Al/Si Solar Cell and Enhancement its Efficiency Via Al-Doping", Nano Biomed. Eng., 2019, Vol. 11, Iss. 2, 170-177.
- [20] Akeel Shakir Alkelaby, Khalid Haneen Abass, Tahseen H. Mubarak, Nadir Fadhil Habubi, Sami Salman Chiad, and Ismaeel Al-Baidhany, "Effect of MnCl₂ Additive on Optical and Dispersion Parameters of Poly methyl Methacrylate Films", Journal of Global Pharma Technology, 2019, Vol. 11, Issue 04, 347-352.
- [21] L. Li, J. Liu, Y. Su, G. Li, X. Chen, X. Qiu, T. Yan, Surface doping for photocatalytic purposes: relations between particle size, surface modifications, and photoactivity of SnO₂:Zn⁺² nanocrystals, Nanotechnology. 20(18), 155706 – 155709 (2009).
- [22] M. F. Khan et al., Nuclear Instruments and Methods in Physics Research Section B: Beam Interactions with Materials and Atoms 368, 45 (2016).
- [23] A. A. Khadayeir, Khalid Haneen Abass, S. S. Chiad, M. Kh. Mohammed, N. F. Habubi, T. Kh.

- Hameed, and I. A. Al-Baidhany, "Study the influence of Antimony Trioxide (Sb_2O_3) on optical properties of (PVA-PVP) composite", Journal of Engineering and Applied Sciences, Vol.13, No.22, pp.9689-9692, 2018.
- [24] Duha M A Latif, Sami S Chiad, Muhssen S Erhayief, Khalid H Abass, Nadir F Habubi, and Hadi A Hussin, Effects of FeCl_3 additives on optical parameters of PVA, Journal of Physics: Conf. series, 1003 (2018).
- [25] Xin Yang, Xiaojuan Lian, Shangjun Liu, Chunping Jiang, JingTian, Gang Wang, Jinwei Chen, Ruilin Wang, Appl. Surf. Sci.282,538(2013).
- [26] Nadir F. Habubi, Khalid H. Abass, Chiad Sami S., Duha M A Latif, Jandow N Nidhal, and Ismaeel Al Baidhany, Dispersion Parameters of Polyvinyl Alcohol Films doped with Fe, Journal of Physics: Conf. series, 1003 (2018).
- [27] Sami Salman Chiad, Khalid Haneen Abass, Tahseen H. Mubarak, Nadir Fadhil Habubi, Musaab Khudhur Mohammed, and Abdulhussain A. Khadayeir, "Fabrication and Study the Structure, Optical and Dispersion Parameters of PMMA with InCl_3 Additive", Journal of Global Pharma Technology, 2019, Vol. 11, Issue 04, 369-374.